

Magnetoelastic anomalies in Fe-Ni Invar alloys

P. Mohn and K. Schwarz

Institut für Technische Elektrochemie, Technische Universität Wien, A-1060 Vienna, Getreidemarkt 9/158, Austria

D. Wagner

Theoretische Physik, Ruhr Universität Bochum, D-4630 Bochum, Federal Republic of Germany

(Received 27 August 1990)

The Fe-Ni alloy is simulated by four ordered structures, whose total energies are obtained as a function of volume and magnetic moment by band-structure calculations employing the fixed-spin-moment (FSM) method. An analytic fit of these $E(M, V)$ surfaces is made and permits an interpolation for varying Ni concentration. These parametrized surfaces allow the introduction of the thermodynamics of spin fluctuations. Among others, the following characteristic Invar properties are calculated: the magnetic contribution to the thermal expansion coefficient α_m , the critical pressure for the disappearance of magnetism P_c , the pressure dependence of the Curie temperature dT_C/dP , and the high-field susceptibility. These quantities agree well with experiment, especially their variation with Ni content. The key quantity is α_m , which shows a narrow minimum as a function of the Ni concentration before the $\alpha \rightarrow \gamma$ (bcc \rightarrow fcc) phase transition occurs. Near the Invar composition the large negative contribution α_m compensates the positive phonon part so that the total thermal expansion nearly vanishes near room temperature. The present combination of models provides new insight into the nature of the Invar effect.

I. INTRODUCTION

The explanation of the Invar effect has been a challenge for solid-state physics since Guillaume¹ reported his findings in 1897 that fcc Fe-Ni alloys at a concentration around Fe₆₅Ni₃₅ show almost no thermal expansion at about room temperature and thus this alloy is "invariant".² Since then, many attempts have been made to understand this unique behavior and several models have been proposed, the most prominent being the 2γ state model by Weiss.³ He assumed two magnetically ordered localized states, a ferromagnetic one with a large volume and an antiferromagnetic one with a smaller volume, where the latter can be thermally excited and thus compensates the thermal expansion caused by phonons. This model, however, makes no direct connection with electronic structure theory. Williams *et al.*⁴ used band-structure calculations to give this phenomenological approach a quantum-mechanical basis and to provide an itinerant-electron interpretation. They used an ordered Fe₃Ni structure to simulate the Invar alloy and found that a ferromagnetic ground state has its equilibrium volume at a larger volume than the nonmagnetic state which lies only slightly higher in energy. Furthermore, they have shown that this energy difference depends on the Fe-Ni composition and is small for Fe₃Ni. Such a situation is very similar to an ordinary ferromagnet near the Curie temperature where a paramagnetic energy minimum is very close to the two ferromagnetic minima (with $\pm M$) of the Landau free energy. One may therefore suspect that fluctuations are important in these systems over the whole temperature range $0 \leq T \leq T_C$ and that this mechanism could qualitatively explain the small

thermal expansion and other effects related to Invar. Recently Moroni and Jarlborg⁵ calculated the thermal excitation between these two itinerant magnetic states and found qualitative agreement with experiment. However, the nature of the mixing between these two magnetic states remained unclear in all the models mentioned above.

In a system as complicated as an Invar-alloy, many phenomena occur, such as order-disorder, $\alpha \rightarrow \gamma$ phase transition, deviation from the Slater-Pauling curve, and so on. In a recent review Wassermann has summarized many physical properties and has categorized them into those which are characteristic for Invar alloys and those which are not.⁶

In order to understand the essential properties we first keep the composition fixed and combine quantum-mechanical band-structure results with the thermodynamics of fluctuations of magnetization and volume, so that the effects of finite temperature can be included.⁷ In a second step, parametrization of these results permits the investigation of the important concentration dependence. This combination of different physical models offers an explanation of the unusual properties of Invar-type alloys.

II. MODELS OF FINITE TEMPERATURE MAGNETISM

After the disappointing results of the Stoner theory for treating finite-temperature magnetism, the problem remained unattempted for a long time. In the mid-70's the first self-consistent spin-polarized band-structure calculations of the ground state of transition metals were

performed, using the local spin-density approximation to treat exchange and correlation effects. These calculations yielded satisfactory values for the magnetic moment, the exchange splitting, and the cohesive energy. However, any attempt to explain the finite-temperature behavior from these results failed. Nowadays it has become clear (see e.g., Shimizu's review article⁸) that the problem is caused by imposing the translational symmetry of the spin-density, an assumption which is violated for $T > 0$. This breakdown of the conventional band picture has led to two main directions to go beyond it.

(i) In the Murata-Doniach approach⁹ (also applied in the present paper) the properties of the magnetic systems are described via a Landau-Ginzburg expansion of the free energy. The effect of spin fluctuations is formulated via randomly fluctuating local magnetic moments. Although these local moments $m(\mathbf{r})$ are vectors, the averaging process using Gaussian¹⁰ statistics (valid outside the critical region) leads to scalar quantities $\langle m(\mathbf{r})^2 \rangle$ which simply renormalize the original Landau-Ginzburg expansion. This scheme was successfully applied by Lonzarich and Taillefer¹¹ to ferromagnetic and nearly ferromagnetic metals.

(ii) In the disordered local moment approach, the magnetic moments on individual atoms are allowed to have random orientations in the sense described by Hubbard¹² or Hasegawa.¹³ Pindor *et al.*¹⁴ implemented this model in a self-consistent Korringa-Kohn-Rostoker (KKR) Coherent-Potential-Approximation (CPA) calculation to simulate the magnetic properties of the transition metals at finite temperature. Bloch symmetry is no necessary constraint in the CPA formalism, so that Stauton *et al.*¹⁵ could calculate the temperature-dependent spin density and the wave-vector-dependent susceptibility $\chi(\mathbf{q})$. With their model they obtained Curie temperatures of 1260 and 225 K for iron and nickel which should be compared to the experimental values of 1043 and 630 K, respectively. The discrepancy between their theory and the experiment could be caused by the assumption that directional disorder is complete above T_C , so that effects of short-range order are neglected, but could be important as suggested by Prange and Korenmann¹⁶ and Capellman.¹⁷ The CPA calculations have clearly shown that the density of states remains virtually unchanged for temperatures well above the Curie point.

In both models the dynamics of the thermal excitations of the spin system are described via the susceptibility $\chi(\mathbf{q})$. One finds that the magnitude of the averaged square of the locally fluctuating magnetic moment and the value of the Curie temperature are closely related to the \mathbf{q} -space integral over $\chi(\mathbf{q})$. Since the first-principles KKR-CPA calculation could not determine the Curie temperature in close agreement with experiment, we circumvent this problem by using the Landau-Ginzburg model in which $\chi(\mathbf{q})$ is approximated by

$$\chi(\mathbf{q}) = \chi_0(1 + \sigma^2 \mathbf{q}^2)^{-1},$$

where $\chi_0 = \chi(\mathbf{q} = 0)$ is the exchange-enhanced susceptibility of the ground state and σ is the real-space parameter¹⁸ which is related to the correlation length and can be

determined from neutron-diffraction experiments. In this approximation the \mathbf{q} -space integral diverges so that its value has to be made finite by introducing a cutoff vector \mathbf{q}_c . With this choice, both the fluctuating magnetic moment and the Curie temperature depend directly on \mathbf{q}_c . In a number of applications of spin fluctuation theory, \mathbf{q}_c has been used as an adjustable parameter to fit experiments (see Ref. 8 and references therein).

All these results justify the combination of ground-state quantum-mechanical calculations at $T = 0$ with a finite-temperature Landau-Ginzburg model as presented here. We combine the best part of both models: the ground-state properties are determined via a parameter-free first-principles band calculation, whose results enter the thermodynamical description of the fluctuations which are scaled by a single parameter \mathbf{q}_c fitted to the experimental T_C .

III. FIXED-SPIN MOMENT CALCULATIONS AND SPIN FLUCTUATIONS

The spin-density-functional theory has shown that the total energy of a system is rigorously defined when the spin-density is known. Practical application of this theory in the form of band-structure calculations (using the local spin-density approximation) yields the well-established Stoner theory of itinerant magnetism which works well at $T = 0$ K. This quantum-mechanical treatment was extended by the fixed-spin-moment (FSM) method^{19,20} which allows us to compute the total energy as a function of magnetic moment and volume.

An analytic treatment of the magnetovolume effects within the Landau theory of phase transitions requires that such energy surfaces $E(M, V)$ are fitted to a polynomial in the bulk magnetization M and the volume V :

$$E(M, V) = E_0 + AM^2 + BM^4 + \beta V + \gamma V^2 + \delta M^2 V, \quad (1)$$

where the number of parameters is kept to a minimum so that they are directly related to physical properties. Since the energy can be taken with respect to E_0 only five parameters are needed to describe most systems. The quality of such a fit has been demonstrated by Entel *et al.*²¹ who could reproduce such energy surfaces to within 0.1 mRy in the important M, V range.

In order to introduce the effects of finite temperature, Wagner²² has shown how to combine quantum-mechanically derived FSM results with a thermodynamic model of locally fluctuating magnetic moments. His ansatz includes both longitudinal and transverse magnetic, as well as volume fluctuations, and thus goes beyond the pioneering work by Murata and Doniach⁹ who assumed only longitudinal magnetic fluctuations.

Wagner²² has obtained a formula for the free energy [see Eqs. (5)–(7) of Ref. 22], but here we keep only those terms which depend on M and V and thus enter the equations of state. This part of the free energy is denoted ΔF :

$$\begin{aligned} \Delta F = & A \langle M^2 + 2 \langle m_{\perp}^2 \rangle + \langle m_{\parallel}^2 \rangle \rangle \\ & + B [M^4 + M^2 (6 \langle m_{\parallel}^2 \rangle + 4 \langle m_{\perp}^2 \rangle) + 8 \langle m_{\perp}^2 \rangle^2 \\ & + 3 \langle m_{\parallel}^2 \rangle^2 + 4 \langle m_{\perp}^2 \rangle \langle m_{\parallel}^2 \rangle] \\ & + E_0 + \beta V + \gamma V^2 + \delta V (M^2 + 2 \langle m_{\perp}^2 \rangle + \langle m_{\parallel}^2 \rangle). \end{aligned} \quad (2)$$

The equations of state for the magnetic field H and the pressure P become

$$H = 2AM + 4BM^3 + 2BM(6 \langle m_{\parallel}^2 \rangle + 4 \langle m_{\perp}^2 \rangle) + 2\delta VM, \quad (3)$$

$$-P = \beta + 2\gamma V + \delta(M^2 + 2 \langle m_{\perp}^2 \rangle + \langle m_{\parallel}^2 \rangle). \quad (4)$$

At the Curie temperature T_C , the bulk magnetization M vanishes and $\langle m_{\parallel}^2 \rangle$ and $\langle m_{\perp}^2 \rangle$, the longitudinal and transverse magnetic fluctuations, become equal. From this condition we calculate the value of the mean-square of the fluctuating magnetic moment $\langle m_c^2 \rangle$ at T_C to be

$$\langle m_c^2 \rangle = \frac{2\gamma A - \delta(\beta + P)}{3\delta^2 - 20\gamma B}. \quad (5)$$

Previously we have applied Wagner's formalism²² to the Fe₃Ni case and have solved it numerically.⁷ It was found that $\langle m_{\perp, \parallel}^2 \rangle$ varies (to a good approximation) linearly with temperature and that the transverse and longitudinal fluctuations $\langle m_{\perp}^2 \rangle$ and $\langle m_{\parallel}^2 \rangle$ are essentially equal over the whole temperature range. This leads to the simplified ansatz

$$\langle m_{\perp, \parallel}^2 \rangle = \langle m_c^2 \rangle (P=0) \frac{T}{T_C(P=0)} = \langle m_c^2 \rangle (P) \frac{T}{T_C(P)}. \quad (6)$$

Since $\langle m^2 \rangle$ is a purely local quantity it may be assumed that the linear dependence on temperature of $\langle m^2 \rangle$ is not changed by changing the pressure or the strength of the magnetic field. It turns out that, in a self-consistent treatment, this approximation is equivalent to neglecting the small dependence of the fluctuations on the magnetization M .

The minor loss in accuracy of this simpler approach with respect to the numerical treatment is by far compensated by the advantage of obtaining analytic solutions. Within these approximations the following five properties can be derived easily.

(i) The magnetic contribution to the thermal expansion coefficient $\alpha_m(T)$ is defined as

$$\alpha_m(T) = \frac{1}{3V} \frac{dV}{dT} = \frac{1}{3} \frac{4B\delta \langle m_c^2 \rangle / T_C}{A\delta - 2B(\beta + P) + 4B\delta \langle m_c^2 \rangle^2 T / T_C}; \quad (7)$$

some authors make use of a slightly different definition of the thermal expansion coefficient by relating the volume change to the volume V_0 (at $T=0$) instead of V as in Eq. (7). With this alternative definition α_m becomes independent of temperature and reads

$$\alpha_m = \frac{1}{3V_0} \frac{dV}{dT} = \frac{1}{3} \frac{4B\delta \langle m_c^2 \rangle / T_C}{A\delta - 2B(\beta + P)}. \quad (8)$$

(ii) The critical pressure for the disappearance of magnetism

$$P_c = \frac{2\gamma A - \beta\delta}{\delta}. \quad (9)$$

(iii) The pressure dependence of the Curie temperature which follows from the assumed pressure independence of $\langle m_c^2 \rangle / T_C$ [Eq. (6)]:

$$\frac{dT_C}{dP} = -\frac{T_C}{P_c}. \quad (10)$$

(iv) The high-field susceptibility χ_{hf} taken at constant pressure

$$\begin{aligned} \chi_{\text{hf}} &= \chi_P = \chi_V \eta, \\ \chi_P^{-1} &= -\frac{2\delta}{\gamma} P_c \left[1 - \frac{T}{T_C} \right], \\ \chi_V^{-1} &= 8BM^2, \\ \eta &= \left[1 - \frac{\delta^2}{4B\gamma} \right]^{-1}, \end{aligned} \quad (11)$$

where χ_V is the susceptibility at constant volume, and η is a temperature-independent magnetomechanical enhancement factor. The importance of the magnetomechanical susceptibility enhancement has already been recognized by Shimizu⁸ who has shown that, for the Fe-Ni system, η becomes anomalously large in the vicinity of the Invar composition.

(v) The forced magnetostriction h :

$$\begin{aligned} h &= \frac{d\omega}{dH} = \frac{1}{V} \frac{dV}{dH} = \frac{1}{V} \frac{dV}{dM} \frac{dM}{dH} \Big|_P = \frac{d\omega}{dM} \frac{dM}{dH} \Big|_P \\ &= -\frac{\delta M}{\gamma V} \chi_P, \end{aligned} \quad (12)$$

which reduces for $T=P=H=0$ according Eq. (11) to

$$h = \frac{M_0}{2V_0} P_c^{-1}. \quad (13)$$

Note that all quantities defined by Eqs. (5)–(13) depend essentially on the *ground-state properties* of the system, i.e., on quantities which are available from FSM band-structure calculations, while the magnetic fluctuations scale according to Eq. (6) with the Curie temperature T_C , which must be taken from experiment.

IV. APPLICATION TO THE Fe-Ni INVARI SYSTEM

The Invar effect occurs only in a relatively small concentration range of the Fe-Ni alloy. Since order-disorder should not play a crucial role,⁶ the following ordered structures (based on the fcc lattice) can represent the Ni concentrations of 0, 25, 50, and 100 at. %, respectively: fcc Fe, Fe₃Ni (Cu₃Au structure), FeNi (CuAu structure), and fcc Ni. The FSM energy surfaces $E(M, V)$ of these

systems were partly recalculated²³ and are shown in Fig. 1. The case of fcc Fe has been investigated in detail by Moruzzi *et al.*²⁴ who predicted a metastable magnetic state at an expanded volume. As Ni is added, a ferromagnetic state evolves (starting near Fe₃Ni) which becomes progressively more stable (towards FeNi) and has a smaller susceptibility. The difference in volume between the nonmagnetic (at $M=0$) and the magnetic (ground) state ΔV_M is found to be large in the latter two cases (25 and 50 % Ni) in contrast to fcc Ni, where it is extremely small. The energy difference between these two minima ΔE_B (ferromagnetic versus nonmagnetic) and their respective ΔV_M are given in Table I. Fe₃Ni is close to the actual Fe₆₅Ni₃₅ Invar composition and exhibits most of the Invar properties,⁷ which require a small ΔE_B but a large ΔV_M , where the latter condition is not found in fcc Ni.

The fit of these four energy surfaces according to Eq. (1) yields five fit parameters as a function of the Ni concentration (Table I) where those connected to the volume

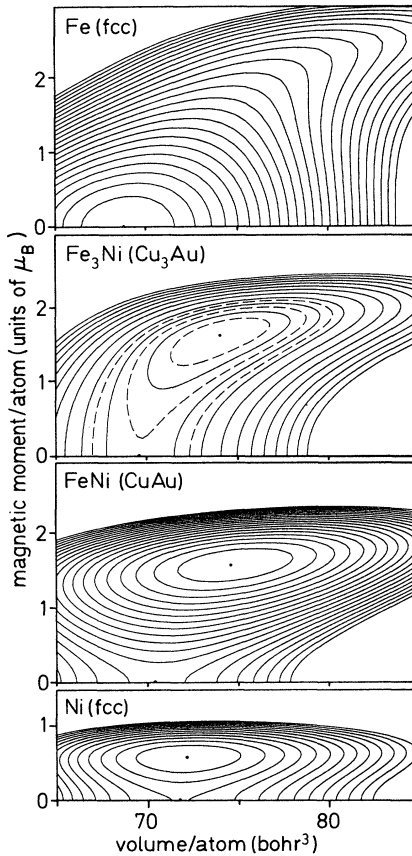


FIG. 1. FSM total energy $E(M, V)$ as a function of volume and magnetic moment of the four systems investigated. All plots are drawn on the same scale and all quantities are normalized to one atom per unit cell. The distance between contour lines is 1 mRy (solid lines) with additional (dashed) lines at 0.5 mRy shown in Fe₃Ni.

TABLE I. Parameters (top panel) of the polynomial fit given in Eq. (1) whose units are such that, by entering the magnetic moment in μ_B and the volume bohr³, the energy is obtained in Ry. Bottom panel: ΔE_M is the energy difference between the nonmagnetic and the magnetic state, ΔV_M is the respective difference in volume. P_c is the critical pressure for the disappearance of magnetism, and T_C is the experimental Curie temperature (Ref. 6).

	fcc Fe	Fe ₃ Ni	FeNi	fcc Ni
$A (\times 10^{-1})$	0.3374	0.2373	0.1728	-0.05188
$B (\times 10^{-3})$	0.2967	0.5423	2.239	23.88
$\beta (\times 10^{-1})$	-0.1995	-0.1408	-0.1602	-0.1823
$\gamma (\times 10^{-3})$	0.1437	0.1012	0.1134	0.1265
$\delta (\times 10^{-3})$	-0.4475	-0.3581	-0.3844	-0.1614
ΔE_B (mRy)		1.57	12.73	2.97
ΔV_M (bohr ³)		-4.54	-4.37	-0.21
P_c (Mbar)		0.10	0.85	4.1
T_C (K)		560	820	630

vary moderately, but the values A and B , describing the magnetic behavior, exhibit a strong dependence on the Ni concentration. In particular, A changes in value and sign since it is related to the inverse susceptibility, and thus must describe the drastic change from a paramagnet for fcc Fe, a very weak itinerant magnet for Fe₃Ni and a strong ferromagnet for FeNi and Ni. In order to account for the important concentration dependence, these five parameters are interpolated by a second-order polynomial in the Ni concentration (between 0 and 50 % Ni).

With these interpolated parameters, our fluctuation model is applied and the various quantities described above are calculated. We start with the discussion of P_c (Fig. 2): the observation that ferromagnetism is lost for low Ni concentrations (around 20 at. % Ni) is already apparent from the top three panels of Fig. 1, where the minimum moves from finite moments for FeNi and Fe₃Ni to $M=0$ for fcc Fe. If the fcc phase would exist over the

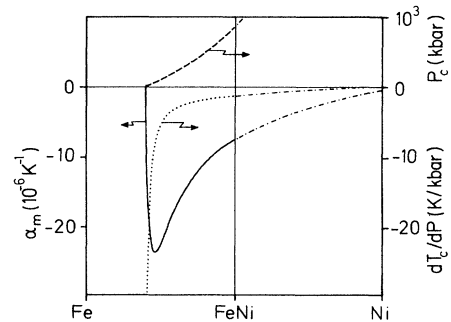


FIG. 2. Magnetic contribution to the thermal expansion coefficient α_m (solid curve), critical pressure P_c (dashed curve), and pressure dependence of the Curie temperature dT_C/dP (dotted curve). The dashed-dotted curves show the extrapolation to the respective values for pure Ni.

whole concentration range, the Fe-Ni alloy would undergo a transition from a magnetic to a nonmagnetic state. However, before the magnetic moment vanishes, a phase transition to bcc ($\gamma \rightarrow \alpha$) occurs which stabilizes the moment again, but this transition is not included in the present study. In our model P_c is given by $-2\Delta E_B/\Delta V_M$ and thus does *not* depend on the actual value of the Curie temperature, but is entirely determined by the FSM results. The ΔV_M and ΔE_B values indicate the different behavior of the three systems and lead to a strong variation of P_c with the Ni concentration (Table I). For Fe₃Ni and fcc Ni, ΔE_B is of the same order of magnitude, but the extremely small value of ΔV_M for Ni brings its critical pressure up to more than 4 Mbar. The ΔV_M value is almost the same for Fe₃Ni and FeNi, but the much higher stabilization energy of FeNi increases P_c with respect to Fe₃Ni.

The most striking result is found for α_m which shows a narrow minimum near the Invar composition (Fig. 2). Our lowest value is $-23 \times 10^{-6} \text{ K}^{-1}$ (at 300 K) (for 27 at. % Ni) in fair agreement with the experimental estimate⁶ of about $-15 \times 10^{-6} \text{ K}^{-1}$ (for 35 at. % Ni). Kakehashi²⁵ calculated the thermal expansion of the Fe-Ni system by using the Liberman-Pettifor²⁶ virial theorem and a CPA static approximation in the functional integral method.¹² His results for α_m as a function of the Ni concentration are very similar to the present work.

The third quantity shown in Fig. 2 is the pressure dependence of the Curie temperature dT_C/dP which is large and negative near the Invar composition and has a value of about -5.5 K/kbar close to the experimental value of -5.0 K/kbar .⁶ Although dT_C/dP is scaled by the Curie temperature (taken from experiment, see Table I), we obtain the same dependence on the Ni concentration as the experiment (see Fig. 26 of Ref. 6). The two quantities α_m and dT_C/dP were also evaluated for Ni and are connected to the corresponding values for FeNi by smooth curves (intermediate values were not computed).

Wassermann⁶ lists two other properties to be charac-

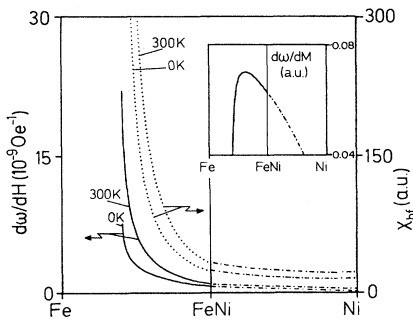


FIG. 3. Forced magnetostriction $h = d\omega/dH$ (solid curve), and high-field susceptibility χ_{hf} (dotted curve). For the inset see text. The dashed-dotted curves show the extrapolation to the respective values for pure Ni.

teristic for Invar alloys: the high-field susceptibility χ_{hf} and the forced magnetostriction $h = d\omega/dH$, both of which should be anomalous, since they are strongly enhanced at room temperature. In Fig. 3 we show them at $T=0$ and 300 K and find that the respective 300-K curves rise much faster in the Invar region than they do at larger Ni concentrations. From Eqs. (11) and (13) one sees that the behavior of both quantities can be traced to the small value of the critical pressure P_c in the Invar region (see also Table I). The actual values compare well in trend with experiment (see Fig. 10 of Ref. 27). For the divergence at low Ni concentrations, the same argument concerning the $\gamma \rightarrow \alpha$ phase transition, as given above, is valid. Although the ground-state property $d\omega/dM$ (inset in Fig. 3) shows a pronounced maximum around the Invar composition, this feature is not seen in the forced magnetostriction, since h is dominated by the sharply rising susceptibility χ_p according to Eq. (12).

The quantity $d\omega/dM$ determines the thermal expansion coefficient α_m when it is written as

$$\alpha_m = \frac{1}{3} \frac{1}{V} \frac{dV}{dT} = \frac{1}{3} \frac{d\omega}{dT} = \frac{1}{3} \frac{d\omega}{dM} \frac{dM}{dT} \Big|_P$$

$$= \frac{1}{3T_C} \left[\frac{T}{T_C} + \frac{P - P_1}{P_0} \left(\frac{P_0 + \frac{5}{2}P_c}{P_0 + P_c} \right) \right]^{-1}, \quad (14)$$

where $P_1 = 2\gamma V_0$ is the bulk modulus of the magnetic ground state and P_0 is the pressure required to force the paramagnetic system to change from volume V_0 to volume V_1 , thus given by $P_0 = -\beta(V_0/V_1 - 1)$. Equation (14) does not only show the influence of the external pressure P , but also accounts for the fact that for some systems the magnetic contribution to the thermal expansion coefficient changes sign at finite temperatures below T_C .

In Eq. (14) dM/dT varies moderately so that the maximum in $d\omega/dM$ leads to the minimum in α_m (Fig. 2) and thus $d\omega/dM$ is an important quantity for the Invar behavior. Rewriting Eq. (14) gives an expression for the spontaneous magnetostriction

$$\omega_{s0} = 3 \int_{T_1}^{T=0} \alpha(T) dT = -\ln \left[1 + \gamma \frac{T_1}{T_C} \right], \quad (15)$$

where $\alpha(T)$ is taken from Eq. (7). The parameter γ

$$\lambda = \frac{4B\delta \langle m_c^2 \rangle}{A\delta - 2B(\beta + P)} = \left[\frac{P - P_1}{P_0} \left(\frac{P_0 + \frac{5}{2}P_c}{P_0 + P_c} \right) \right]^{-1} \quad (16)$$

is a quantity which is specific for a material. For Fe₃Ni we obtain a value of $\lambda = -0.04$ for $P=0$. From Eq. (15) taking T_1 near room temperature (300 K), we find $\omega_{s0} = 2.2 \times 10^{-2}$ which is in good agreement with the value of 1.9×10^{-2} estimated experimentally.⁶

V. SPIN FLUCTUATIONS AND THE FREE ENERGY

The introduction of spin fluctuations in a Landau-Ginzburg free-energy expression leads to a spin-fluctuation-dependent contribution to the free energy ΔF

as was defined in Eq. (2). To study how ΔF changes with temperature, we have to employ Eqs. (3)–(6) as follows: The amplitude of the fluctuating magnetic moment at T_C is given by Eq. (5), its value for a temperature $T \neq T_C$ is obtained from the scaling relation [Eq. (6)]. With this value we enter the equations of state [Eqs. (3) and (4)] and obtain M and V for the respective P and H . With these values for M , V , and $\langle m^2 \rangle$, we calculate the free-energy contribution as energy surfaces $\Delta F(M, V)$. Four such surfaces are shown in Fig. 4 for $T=0$, $T=0.5T_C$,

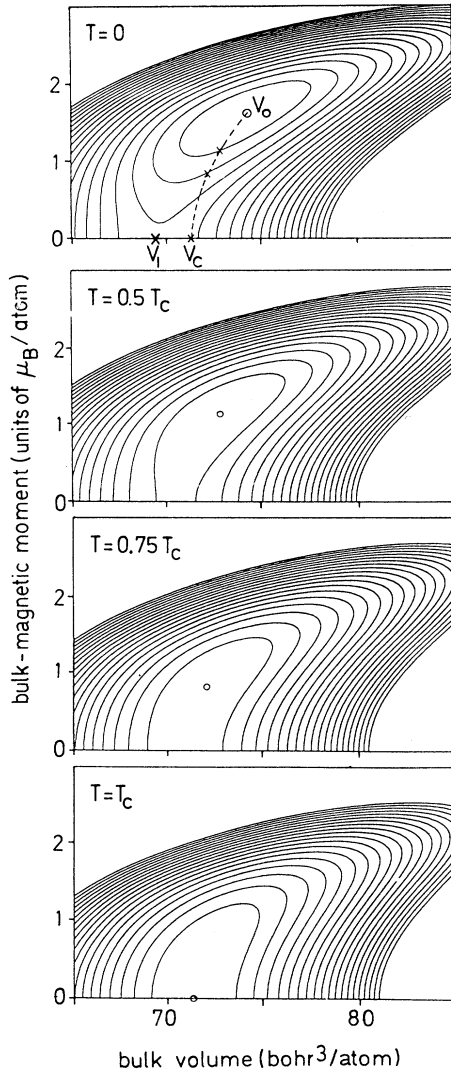


FIG. 4. The free-energy contribution ΔF [Eq. (2)] as a function of the bulk-magnetization M and the bulk volume V (the distance between the contour lines is 0.5 mRy). The four plots are calculated for four different temperatures up to T_C . The dashed line in the top panel shows how the equilibrium values of M and V evolve with temperature, where the crosses indicate the minima corresponding to the three panels below.

$T=0.75T_C$, and $T=T_C$. The $T=0$ surface is the FSM result from the band calculation. For $P=H=0$ one obtains the equilibrium at a volume V_0 and a finite bulk magnetic moment M_0 . Any deviation from this equilibrium is connected with an external pressure P and an external magnetic field H which are included as constraints within the FSM self-consistency cycle. Our free-energy formulation of the magnetomechanical properties allows the same interpretation for the finite-temperature case, i.e., the equilibrium (given by the small circles) is obtained for zero pressure and zero field. The surfaces show the behavior of the system for finite external P and H at a temperature T . From the series of plots shown in Fig. 4, it can be clearly seen how the free energy is changed continuously as the amplitude of the locally fluctuating magnetic moments increases.

In the top panel of Fig. 4 we have marked three different volumes, namely, V_c the equilibrium volume at $T=0$, V_1 the equilibrium volume of the Stoner paramagnetic state, and V_c the volume at the Curie temperature as calculated from the present spin-fluctuation model. The fact that V_c is larger than V_1 is caused by locally fluctuating magnetic moments which exist even at a temperature where the bulk magnetization M has already vanished. This means that spin fluctuations reduce the spontaneous volume magnetostriction considerably and thus correct the shortcoming of the Stoner model. In an earlier paper²⁸ this feature has been formulated via an internal pressure exerted by the spin fluctuations.

The renormalization of the Landau-Ginzburg parameters by the spin-fluctuation terms yields an itinerant electron description of the Invar effect. This is made possible by the weakly itinerant behavior of the Fe-Ni alloy in the Invar region. Weak itinerant magnetism is characterized by a large susceptibility χ_{hf} and a small ratio M_0/N , where M_0 is the equilibrium moment, and N the average number of d electrons per atom. In case of Fe_3Ni this ratio is ≈ 0.25 , a value sufficiently small to yield convergence of the Landau-Ginzburg expansion.

VI. CONCLUSION

In the Fe-Ni system it is important to investigate how various physical properties which are characteristic for Invar alloys depend on the Ni concentration. This is made possible by simply interpolating the five parameters which characterize the $E(M, V)$ surfaces for 0, 25, and 50 at. % Ni. Although we find the Invar behavior at a smaller Ni concentration than the actual $\text{Fe}_{65}\text{Ni}_{35}$, our model reproduces the concentration dependences in good semiquantitative agreement with experimental data.

Our phenomenological theory is based on first-principles calculations which include exchange and correlation effects via the spin-density-functional theory. The FSM model allows us to retain this effective many-body treatment by computing the total energy as a function of M and V . The combination of quantum mechanics (band structure) and a classical thermodynamic treatment of fluctuations yields a simple model to describe the anomalous behavior of Fe-Ni Invar. In a system with a shallow energy surface (in volume and magnetic moment), spin

and volume⁷ fluctuations are essential for an understanding of the magnetovolume effects. With rising temperature, the fluctuations modify this effective energy surface continuously and concomitantly change the average volume and magnetic moment. The formulation via a renormalization of the Landau-Ginzburg coefficients of the ground state describes the influence of the spin fluctuations on microscopic quantities (such as the susceptibility) which are directly related to the band structure. With these quantities we calculate the thermodynamic variables from a "ground state" for which finite temperature is an external constraint. In this sense our description of the thermal properties of magnetic systems is comparable to the disordered local moment model²⁹ where the local moments affect the electronic states and thus the related macroscopic thermodynamic quantities. Both our model and the disordered local moment scheme describe fluctuations on a microscopic level in contrast to previous theoretical attempts which rely on a mixed magnetic state being composed either of two localized³ or two itinerant^{4,5} magnetic states (phases) between which thermal excitations are assumed.

The characteristic Invar quantities can be expressed in

terms of the FSM energy surface which, in the present analytic representation, requires five parameters. For a ferromagnetic system there exists a minimum with M_0 and V_0 and a saddle point at $M=0$ with V_1 . Together with the energy difference of these two special points and the bulk modulus (at $M=0$ and V_1) the five parameters of the FSM surface are determined. Only cases near a magnetic instability could lead to Invar behavior which requires a small ΔE_B and a large ΔV_M as found in the Fe-Ni system for certain Ni concentrations. In a more general situation, a flat energy surface between two minima at different moments (and volumes) could also cause the Invar effect, which could occur in the Fe-Pt system where recent experiments found evidence for a pressure-induced transition from a high-moment to a low-moment state.³⁰

ACKNOWLEDGMENTS

The authors wish to thank both Dr. V. L. Moruzzi for providing us with the accurate energy surface of Fe₃Ni and M. Thon for critical comments.

¹Ch. E. Guillaume, C. R. Acad. Sci. Paris **125**, 235 (1987).

²For recent developments see, for example, Proceedings of the ISOMES '89 International Symposium on Magnetoelasticity and Electronic Structure of Transition Metals, Alloys and Films, Duisburg, 1989 [Physica B **161** (1989)].

³R. J. Weiss, Proc. R. Soc. London **82**, 281 (1963).

⁴A. R. Williams, V. L. Moruzzi, C. D. Gelatt, Jr., J. Kübler, and K. Schwarz, J. Appl. Phys. **53**, 2019 (1982).

⁵E. G. Moroni and T. Jarlborg, Phys. Rev. B **41**, 9600 (1990).

⁶E. F. Wassermann, in *Invar: Moment-Volume Instabilities in Transition Metals and Alloys*, Vol. 5 of *Ferromagnetic Materials*, edited by K. H. Buschow and E. P. Wohlfarth (North-Holland, Amsterdam, 1990).

⁷P. Mohn, K. Schwarz, and D. Wagner, Physica B **161**, 153 (1989).

⁸M. Shimizu, Rep. Prog. Phys. **44**, 329 (1981).

⁹K. K. Murata and S. Doniach, Phys. Rev. Lett. **29**, 285 (1972).

¹⁰T. Moriya, J. Magn. Magn. Mater. **14**, 1 (1979).

¹¹G. G. Lonzarich, and L. Taillefer, J. Phys. C **18**, 4339 (1985).

¹²J. Hubbard, Phys. Rev. B **19**, 2626 (1979); **20**, 4584 (1979).

¹³H. Hasegawa, J. Phys. Soc. Jpn. **49**, 963 (1980).

¹⁴A. J. Pindor, J. Staunton, G. M. Stocks, and H. Winter, J. Phys. F **13**, 979 (1983).

¹⁵J. Staunton, B. L. Gyorffy, A. J. Pindor, G. M. Stocks, and H. Winter, J. Magn. Magn. Mater. **45**, 15 (1984).

¹⁶R. E. Prange and V. Korenmann, Phys. Rev. B **19**, 4961 (1979).

¹⁷H. Capellman, Z. Phys. B **34**, 29 (1979).

¹⁸E. Stenzel and H. Winter, J. Phys. F **16**, 1789 (1986).

¹⁹A. R. Williams, V. L. Moruzzi, J. Kübler, and K. Schwarz, Bull. Am. Phys. Soc. **29**, 278 (1984).

²⁰K. Schwarz and P. Mohn, J. Phys. F **14**, L 129 (1984).

²¹P. Entel and M. Schröter, J. Phys. (Paris) Colloq. **8**, 293 (1988).

²²D. Wagner, J. Phys. Condens. Matter **1**, 4635 (1989).

²³V. L. Moruzzi (private communication).

²⁴V. L. Moruzzi, P. M. Marcus, K. Schwarz, and P. Mohn Phys. Rev. B **34**, 1784 (1986).

²⁵Y. Kakehashi, J. Phys. Soc. Jpn. **49**, 2421 (1980).

²⁶D. G. Pettifor, J. Phys. F **8**, 219 (1978).

²⁷E. F. Wassermann, Solid State Phys. **27**, 85, (1987).

²⁸P. Mohn, D. Wagner, and E. P. Wohlfarth, J. Phys. F **11**, L13 (1987).

²⁹H. Hasegawa, J. Phys. C **14**, 2793 (1981).

³⁰M. N. Abd-Elmeguid and H. Micklitz, Phys. Rev. B **40**, 7395 (1989).